TWO-PHASE FLOW THROUGH DIFFUSERS

Mofreh H. Hamed

Mechanical Power Engineering Department,
Faculty of Engineering, Menoufia University, Egypt

ABSTRACT

This paper describes a theoretical model for the solution of steady one-dimensional dispersed two-phase flow of wet steam in diffusers. Effects of initial flow conditions such as, slip coefficient, wetness fraction, droplet radius and diffuser geometry parameters on the flow characteristics are considered. Predictions of flow parameters for continuous-phase and discrete-phase are obtained using Runge-Kutta method in solving the theoretical model. The results of calculations of flow of wet steam through diffusers detect a great variation in the diffuser performance, and show that this great variation depends upon the interaction processes between the two-phases assembly. Also the results show that the presence of convergent section during flow of wet steam through diffusers at certain conditions may lead to critical feature and depends upon the dryness fraction. A comparison between predictions of the present model and other published analytical and experimental results are held. The comparison indicates a good qualitative agreement between the results of the present model and the others and that both sets have the same trend.

Keywords: Two-phase, Diffuser, Slip coefficient, Heat transfer, Wet steam.

INTRODUCTION

Flow in diffusers is of considerable practical importance in turbines, pumps, fans, compressors and other roto-dynamic machines. At some stages of the passage through the machine there arises the problem of recovering kinetic energy, which cannot be sacrificed without detrimental effect on their efficiency. The kinetic energy is converted to pressure energy by decelerating the flow in diffusers of suitable contour, making it necessary to examine in detail their performance.

Recent research on subsonic diffusers with single-phase flow has greatly increased the understanding of internal flows with adverse pressure gradients, and the variables, which control diffuser performance [1-3]. The flow of two-phase diffuser research can be found in many engineering problems, e.g., design of gas-driven jet pumps, a draft tube of a cross-flow water turbines and evaluation of two-phase flow properties in diffusers which, has been considered as one of the greatest importance of these problems.

Two-dimensional diffuser performance with subsonic, two-phase, air-water mixture flow has been investigated by Hench and Johnston [4]. They studied experimentally the performance of a vertical rectangular diffuser and showed that diffusers with air-water mixture have the same general performance as diffusers with a single-phase. Tomitaro and Kenichi [5] studied also experimentally the performance of a vertical diffuser for air-water mixture. The diffuser performance with air-water mixture is affected not only by the channel profile but also by the inlet flow velocity profile. They also concluded that, the efficiency of the diffuser deteriorates as the air-water ratio increases. Some effects on conical diffuser performance of preceding normal shock boundary-layer interaction were done by Livesey and Odukwe [6]. The experimental

results are presented for the variation of static pressure rise coefficient, the transformation efficiency and the total loss coefficient. Therefore, it appeared from the literature review that the study of two-phase flow in a diffuser has not received the attention of many investigators; so the nature of diffuser performance with two-phase fluid flow is not well established and publications which concerning the theoretical treatment of two-phase flow with inter-phase slip and heat transfer are needed.

State of meta-stable in flow of wet steam occurs, rapidly or slowly due to hetro-phase fluctuation, and more flow condensation leads to stable or near stable state. This process is depending upon the degree of flow wetness. Therefore, within the above reasons, it is very important to study and analyze two-phase flow of wet steam with different wetness and with other arbitrary initial conditions through diffusers.

The primary incentive for this study is to verify a theoretical model, based on one dimensional, steady mono-dispersed two-phase flow approximations, to simulate the flow through diffuser with variable geometry.

The proposed model uses the basic flow equations developed to study the effect of initial flow conditions such as; slip coefficient, droplet radius and wetness fraction as well as diffuser geometry parameters on the flow characteristics.

GENERAL FLOW EQUATIONS AND CALCULATION PROCEDURE:

Flow Assumptions

To study the mono-dispersed two-phase flow in diffuser shown in Figure 1-a, the following assumptions are taken in deriving the system of equations which govern the flow model:

i- The flow is one-dimensional.

ii- Discrete-phase consists of mono-dispersed incompressible spherical liquid droplets and distributed uniformly through the vapour phase.

iii- Initial flow conditions are corresponding to wet steam condition.

iv- Continuous-phase is treated as an ideal gas.

v- Forces affecting the droplet are, the friction force, pressure gradient, and force due to surface tension.

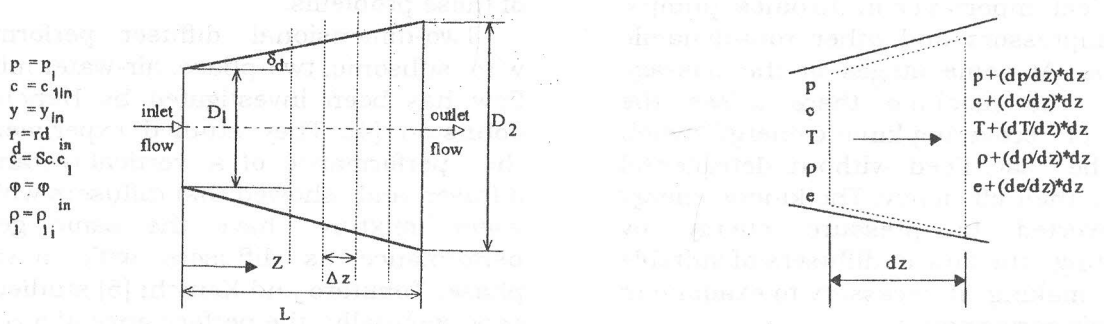

a- Diffuser geometry and initial flow conditions

b- Infinitesimal flow control volume.

Figure 1 One-dimensional flow through a diffuser.

Flow equations

Considering the above assumptions, a system of equations governing the flow model for the two components of the flow, [7] is:

i- For continuous-phase

The equations of conservation of mass, momentum and energy are written as follows:

-Continuity equation:

$$\frac{d\rho_1\varphi_1c_1A}{dz} = -\chi \cdot A \qquad (1)$$

-Momentum equation:

$$\rho_1\varphi_1c_1\frac{dc_1}{dz} = -\chi(c_3 - c_1) - F - \frac{dp_1\varphi_1}{dz} \qquad (2)$$

-Energy equation:

$$\rho_1\varphi_1c_1\frac{di_{o1}}{dz} = -\chi \cdot (i_{o3} - i_{o1}) - Fc_2 + Q - \frac{d\varphi_2c_2p_2}{dz} - \frac{d\varphi_1q_1}{dz} \qquad (3)$$

ii- For discrete-phase

In a similar way, the equations of conservation of mass, momentum and energy for the discrete-phase are written as follows:

-Continuity equation:

$$\frac{d\rho_2\varphi_2c_2A}{dz} = \chi \cdot A \qquad (4)$$

-Momentum equation:

$$\rho_2\varphi_2c_2\frac{dc_2}{dz} = \chi(c_3 - c_2) + F - \frac{dp_2\varphi_2}{dz} \qquad (5)$$

-Energy equation:

$$\rho_2\varphi_2c_2\frac{d(i_{o2} + v_s)}{dz} = \chi \cdot (i_{o3} - i_{o2} - v_s) + Fc_2 - Q + \frac{d\varphi_2c_2p_2}{dz} - \frac{d\varphi_2q_2}{dz} \qquad (6)$$

Auxiliary Equations

To solve the system of equations (1 to 6), the following auxiliary equations are considered:

1-The stagnation enthalpy is calculated as follows:

$$i_{o1} = i_1 + \frac{c_1^2}{2} \qquad (7)$$

$$i_{o2} = i_2 + \frac{c_2^2}{2} \qquad (8)$$

$$i_{o3} = \mu + \frac{c_3^2}{2} \qquad (9)$$

Where, μ and c_3 are defined as follows,

$$\mu = \begin{cases} \mu_1 = i_1 - T_1S_1. & c_3 = c_1 \text{ if } \chi > 0.0. \\ \mu_2 = i_2 - T_2S_2. & c_3 = c_2 \text{ if } \chi < 0.0 \end{cases} \qquad (10)$$

2- Equation of state for continuous-phase is:

$$p_1 = \rho_1 \cdot R_B \cdot T_1, \text{ Where, } R_B = B.R_{ig} \qquad (11)$$

3- The droplet of discrete-phase has a constant density:

$$\rho_2 = \text{const.} \qquad (12)$$

4- Volumetric concentration for the two phases:

$$\varphi_1 + \varphi_2 = 1 \qquad (13)$$

5- Assuming that the continuous-phase is studied as an ideal gas flow, then its enthalpy can be calculated from the following equation:

$$i_1 = \frac{\gamma}{(\gamma - 1)} \cdot \frac{p_1}{\rho_1} + \text{const.} \qquad (14)$$

6- The enthalpy of discrete-phase is:

$$i_2 = f(\rho_2, T_2) \qquad (15)$$

7- The entropy of each phase is calculated as follows:

$$S_1 = S_{1in} + \frac{R_B}{(\gamma - 1)} \ln\left[\frac{p_1}{p_o}\left(\frac{\rho_o}{\rho_1}\right)^{\gamma}\right] \qquad (16)$$

$$S_2 = S_{2in} + c_{v2} \ln\left[\frac{T_2}{T_{o2}}\right] \qquad (17)$$

8- Heat release (Q) is calculated as follows:

$$Q = \frac{\varphi_2}{V_2} S_d \alpha (T_1 - T_2) \qquad (18)$$

Where (α) is the coefficient of heat transfer which is calculated through Nusselt number and defined by; $\alpha = Nu\lambda_1/2r_d$ and the Nusselt number (Nu) is calculated from the following formula as in Reference [7]:

$$Nu = 2 + 0.03Re_{rel.}^{0.54}Pr^{0.38} + 0.35Re_{rel.}^{0.58}Pr^{0.36} \qquad (19)$$

Where, Pr is the Prandtel number and defined as, $(\mu_1 c_{p_1}/\lambda_1)$ and $Re_{rel.}$ is the relative Reynolds number and defined as, $Re_{rel.} = \frac{2r_d|c_1 - c_2|}{\upsilon_1}$, as in Reference 8.

9- Mean heat transfer by conduction through continuous-phase can be represented by:

$$q_1 = -\lambda_1 \frac{dT_1}{dZ} \qquad (20)$$

10- Neglecting the effect of impinging between droplets, then:

$$p_2 = 0$$
$$q_2 = 0 \qquad (21)$$

11-Friction force of droplets is:

$$F = -\varphi_2 \frac{dp_1}{dz} + \frac{\varphi_2}{V_2} S_M C_f \rho_1 |c_1 - c_2|(c_1 - c_2), \quad (22)$$

12-The friction coefficient C_f, is calculated from the following relation [7, 9]:

$$C_f = \frac{24}{Re_{rel.}} + \frac{2.5}{Re_{rel.}^{0.25}} \quad (23)$$

13- Specific energy due surface tension, is defined by:

$$v_s = \frac{3\sigma}{\rho_2 r_d} \quad (24)$$

14- Velocity of phase transformation is defined as:

$$\chi = \frac{\varphi_2}{V_2} \frac{dm_d}{dt} \quad (25)$$

Where, $\frac{dm_d}{dt}$ is the mass velocity change of droplet, which can be expressed as in References [7, 10] by the following relation:

$$\frac{dm_d}{dt} = \frac{4\pi p_1 r_d^2}{\sqrt{2\pi R_B T_1}} \cdot (\alpha_c - \alpha_e \sqrt{\frac{T_1}{T_2}}) \quad (26)$$

15-In the case of gas flow with droplets and there is mass transfer between the two components, therefore, it is of importance to add the equation which govern the growth of spherical droplet radius. This growth can be calculated either from the differentiation of mass of droplet or through the equation which govern ,this growth as follows;

$$m_d = \frac{4}{3}\pi r_d^3 \rho_2 \quad (27)$$

Then,

$$\frac{dr_d}{dt} = \frac{1}{4\pi r_d^2 \rho_2} \frac{dm_d}{dt} \quad (28)$$

$$\frac{d}{dz}(A\rho_2\varphi_2 c_2 r_d) = \frac{4}{3} A \chi r_d \quad (29)$$

To solve the system of equations (1-6) with the help of the above auxiliary equations (7-29), we must put these equations (1-2-4-5-6) respectively in the normalized form as follows:

$$\frac{d\rho_1}{dz} = -\rho_1 (\frac{\chi}{\rho_1 \varphi_1 c_1} + \frac{1}{c_1}\frac{dc_1}{dz} + \frac{1}{\varphi_1}\frac{d\varphi_1}{dz} + \frac{1}{A}\frac{dA}{dz}) \quad (30)$$

$$\frac{dc_1}{dz} = \frac{1}{\rho_1 \varphi_1 c_1}(\chi(c_1 - c_3) - p_1 \frac{d\varphi_1}{dz} - \varphi_1 \frac{dp_1}{dz} - F) \quad (31)$$

$$\frac{d\varphi_1}{dz} = \varphi_2 (-\frac{\chi}{\rho_2 \varphi_2 c_2} + \frac{1}{c_2}\frac{dc_2}{dz} + \frac{1}{A}\frac{dA}{dz}) \quad (32)$$

$$\frac{dc_2}{dz} = \frac{1}{\rho_2 \varphi_2 c_2}(F - \chi(c_2 - c_3)) \quad (33)$$

$$\frac{di_{o2}}{dz} = \frac{1}{\rho_2 \varphi_2 c_2}(\chi(i_{o3} - i_{o2} - v_s) - Q + Fc_2 + \frac{d\varphi_2 c_2 p_2}{dz} - \rho_2 \varphi_2 c_2 \frac{dv_s}{dz}) \quad (34)$$

Finally the pressure gradient term is calculated from Equation 3 as follows:

$$\rho_1 \varphi_1 c_1 [\frac{\partial(i_1 + c_1^2/2)}{dz}] = \chi \cdot (i_{o1} - i_{o3}) - Fc_2 + Q - \frac{d\varphi_2 c_2 p_2}{dz} - \frac{d\varphi_1 q_1}{dz} \quad (35)$$

Where, $i_1 = f(p_1 . \rho_1)$ then,

$$di = \frac{\partial i_1}{dp_1}\Big|_{\rho_1} \frac{dp_1}{dz} + \frac{\partial i_1}{\partial \rho_1}\Big|_{p_1} \frac{d\rho_1}{dz} \quad (36)$$

By differentiating equation 14 yields;

$$\frac{\partial i_1}{dp_1}\Big|_{\rho_1 = c} = \frac{\gamma}{\gamma - 1}\frac{1}{\rho_1} \quad (37)$$

$$\frac{\partial i_1}{\partial \rho_1}\Big|_{p_1 = c} = -\frac{\gamma}{\gamma - 1}\frac{p_1}{\rho_1^2} \quad (38)$$

After rearrangement and substituting Equations 20, 21, 36, 37 and 38 in Equation 35 and also neglecting the heat conduction through continuous-phase, then the pressure gradient can be written in the following form:

$$\frac{dp_1}{dz} = \frac{\chi L_\chi + FL_F + QL_Q + \frac{d\ell nA}{dz} L_A}{\varphi_1 (1 - M_1^2)} \quad (39)$$

Where,

$$L_\chi = c_1[1 - (\frac{c_3}{c_2} - 1)(1 + (\gamma - 1)M_1^2) + \frac{1}{\gamma}\frac{\rho_1 c_1}{\rho_2 c_2}(1 - \frac{1}{M_1^2})(\frac{c_3}{c_2} - 2) + \frac{i_{o3} - i_{o1}}{\frac{\gamma}{\gamma - 1}\frac{p_1}{\rho_1}}]$$

$$L_F = \frac{1}{\gamma}\frac{\rho_1 c_1^2}{\rho_2 c_2^2}(1 - \frac{1}{M_1^2}) + (\gamma - 1)M_1^2(\frac{c_2}{c_1} - 1) - 1$$

$$L_Q = -(\gamma - 1)\frac{M_1^2}{c_1}$$

$$L_A = \gamma p_1 M_1^2 [\varphi_1 + \frac{1}{\gamma}\varphi_2(1 - \frac{1}{M_1^2})]$$

$$M_1^2 = \frac{c_1^2}{\gamma \frac{p_1}{\rho_1}}$$

Method of computational solution

A computer program was built up to solve Equations 29 to 34 and 39 with the help of the auxiliary equations. Numerical integration of these equations is carried out using Runge-Kutta method [11]. This integration was carried out for a duct of known geometry as shown in Figure 1-a with finite step size $\Delta z = L/n$, where n is the number of steps. Through each step of computations, an infinitesimal difference (gradient) for each parameter is calculated for one dimensional flow through infinitesimal control volume, Figure1-b, to obtain a new value for this parameter under the following inlet conditions:

$$Z = 0, \quad y = y_{in}, \quad p_1 = p_{in}, \quad \rho_1 = \rho_{in},$$
$$S_c = S_{cin}, \quad c_1 = c_{1in}, \quad c_2 = S_c \cdot c_{1in}, r_d = r_{din},$$
$$\varphi_{2_{in}} = \frac{y_{in}\rho_1}{\rho_2(1-y_{in})}, \quad \varphi_{1_{in}} = 1 - \varphi_{2_{in}} \quad \text{and}$$
$$T_1(Z=0) = T_2(Z=0) = T_s(Z=0, p = p_{in}) \qquad (40)$$

RESULTS AND DISCUSSION

The dynamics of two-phase flow depend upon heat and mass transfer between the two-phases, which affect all the conservation equations. Also the mechanical interaction between the two-phases affects the equations of momentum and energy. It is lso clear from Equation 39 that all the above parameters affect the pressure gradient. The predictions, presented herein are obtained for mono-dispersed two-phase flow through variable area duct with the profile, shown in Figure 1. The diffuser has a constant inlet diameter, D_1 = 0.098 m and length, L = 0.1 m. The effects of inlet flow conditions and the geometrical parameters on the diffuser performance will be discussed in the following sections. The computations are performed for diffuser half divergence angle of 2, 4, 6 and 8°, initial slip coefficient, 0.5, 0.7, 0.9 and 0.95, for different initial droplet radius varies from 2.5 μm to 10 μm, and also wetness fraction changes from 0 to 0.5.

Axial Static Pressure Distribution

The variations of axial static pressure $(p/p_{in})$of flow of wet steam at variable inlet flow conditions such as wetness fraction, slip coefficient and droplet radius are shown in Figure 2. The distribution of static pressure of flow along the diffuser axis at variable inlet flow wetness and keeping all the other flow parameters constant is shown in Figure 2-a. It is observed from this figure that, increasing the initial flow wetness, causes a variation in the static pressure in the first part of the diffuser with negative pressure gradient, while in the second part of the diffuser, the static pressure gradient has a positive value. This is because in the first region of the diffuser the mechanical influence exceeds the geometrical influence and leads to decrease in the static pressure without regarding to the channel form and subsonic flow condition. At a certain point in the diffuser the mechanical influence equal to the geometrical influence and the pressure will be minimum. After that any increase in the diffuser area, the geometrical influence will exceed the mechanical influence and then the static pressure gradually increases. In general, for high value of initial flow wetness, the diffuser acts as a nozzle up to the middle part of the diffuser, where the pressure takes the minimum value. After that the process characterized an increasing in static pressure, where near the exit section the pressure gradient is dropped. Figure 2-b shows the effect of initial slip coefficient on the static pressure distribution along the diffuser axis. It is seen that as the coefficient of slip increases, the region of negative pressure gradient shrinks and the static pressure at the diffuser exit increases. From this figure it is seen that as the slip coefficient approaches unity the duct completely acts as a diffuser and the presence of nozzle zone diminishes. Figure 2-c shows the effect of droplet radius on the static pressure distribution along the diffuser axis. This figure shows that as the droplet radius decreases and keeping all the other parameters constant, the static pressure sharply decreases in the first part

of the diffuser. This is due to the acceleration of droplet through this part. The results showing the effect of changing diffuser angle (δ_d) are presented in Figure 2-d. The computations are performed for diffusers with half divergence angles of 2, 4, 6 and 8 degrees. The results show that as the half diffuser angle (δ_d) decreases, the length of the first part of the diffuser which acts as a nozzle increases and the exit pressure decreases. This is because the geometrical influence is in the proportional relation with the half diffuser angle, Equation 39. Then, small decreasing in half-diffuser angle will lead to a more decrease in the geometrical influence than the mechanical influence.

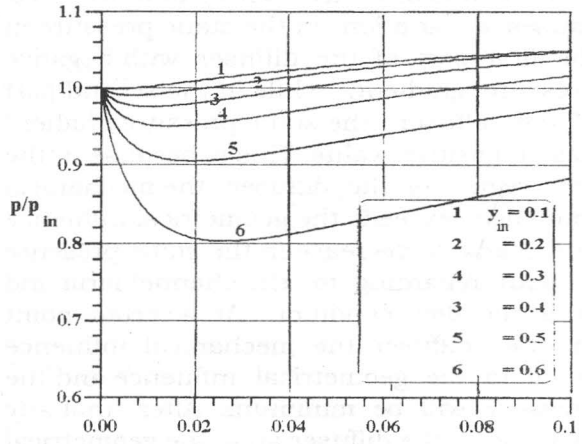

a- Effect of initial wetness fraction, (y_{in})
($r_{d\,in}$ = 5 μm , δ_d = 6° & $S_{c\,in}$ = 0.5)

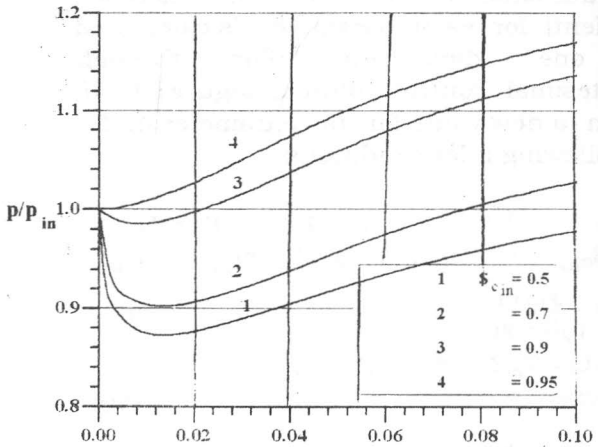

b- Effect of initial slip coefficient, ($S_{c\,in}$)
($r_{d\,in}$ = 2.5 μm , δ_d = 6° & y_{in} = 0.5)

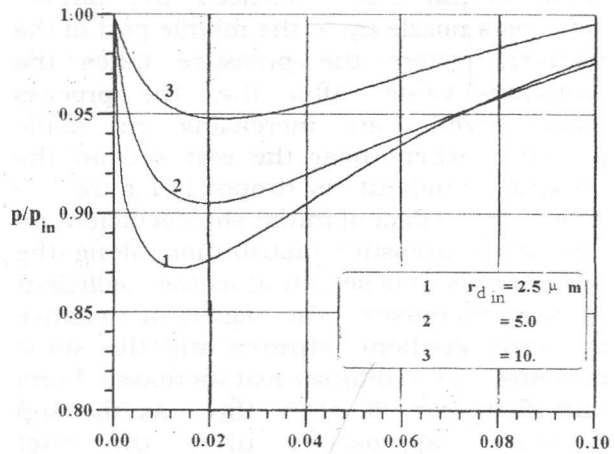

c- Effect of initial droplet radius, ($r_{d\,in}$)
(δ_d = 6° , y_{in} = 0.5 & $S_{c\,in}$ = 0.5)

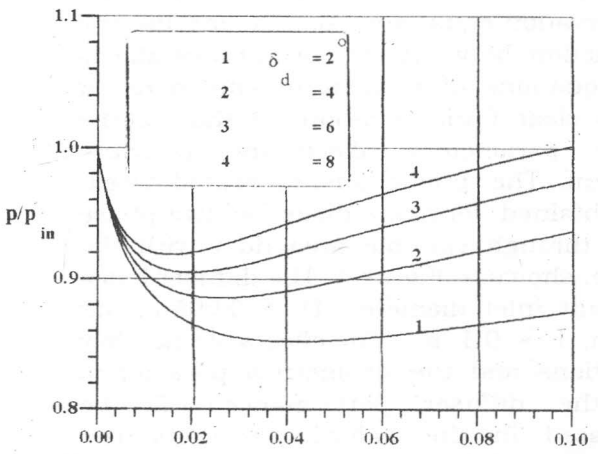

d- Effect of half diffuser angle, (δ_d)
($S_{c\,in}$ = 0.5, y_{in} = 0.5 & $r_{d\,in}$ = 5 μm)

Figure 2 Dimensionless axial static pressure (p/p_{in}) distribution along diffuser axis. (p_{in} = 6 bar & c_{in} = 300 m/s)

Velocity Ratio Between Discrete-Phase and Continuous-Phase of The Flow

The slip coefficient is taken as a parameter in the kinematics similarity between the two phases. Therefore, it is important to study the effect of inlet flow conditions such as initial wetness fraction, inlet slip coefficient, initial droplet radius and half diffuser angle (δ_d) on the velocity ratio between discrete-phase and continuous-phase of the flow. These results are plotted in Figures 3 and 4. The variation of velocity ratio at variable inlet flow wetness and at constant values for all the other flow parameters is shown in Figure 3-a. This figure shows that during flow of wet steam through the diffuser in the case of subsonic flow, the static pressure increases and the velocity of continuous-phase decreases, then the velocity ratio increases at constant wetness fraction. Increasing the initial flow wetness, slowly increase the continuous-phase velocity in the first part of the duct, then the velocity ratio slowly decreases while in the second part of the duct the velocity ratio decreases. This is due to the effect of condensation and evaporation during expansion. As a whole the change in local slip coefficient due to the small change in the wetness fraction is so small. Figure 3-b shows the effect of inlet slip coefficient on the velocity ratio. It is seen from this figure that there is no effect on the velocity ratio along the diffuser axis except at the entrance zone. Figure 3-c shows the effect of inlet droplet radius on the variation of local slip coefficient along the diffuser axis. It is clear that, as the droplet radius decreases, the rate of decrease of velocity (c_1) is more and translated to the discrete phase velocity (c_2), then the local slip coefficient increases. The effect of diffuser half angle (δ_d) on the velocity ratio (c_2/c_1) along the diffuser axis and keeping all the other flow parameters constant is shown in Figure 3-d. On the other side the distribution of the absolute values of velocity for each phase at the same conditions mentioned above is shown in Figure 4. These results indicate clearly that, increasing the diffuser angle causes a decrease in the continuous-phase velocity (c_1) and also in the discrete-phase velocity (c_2), however, the rate of decrease of (c_1) is greater than the rate of decrease of (c_2), this will lead to an increase in the ratio of discrete-phase velocity to continuous-phase velocity (c_2/c_1).

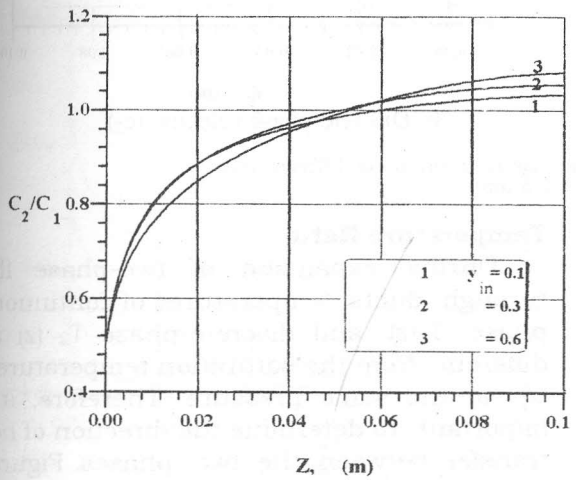

a- Effect of initial wetness fraction, (y_{in})
($r_{d_{in}}$ = 5 μm , δ_d = 6° & $S_{c_{in}}$ = 0.5)

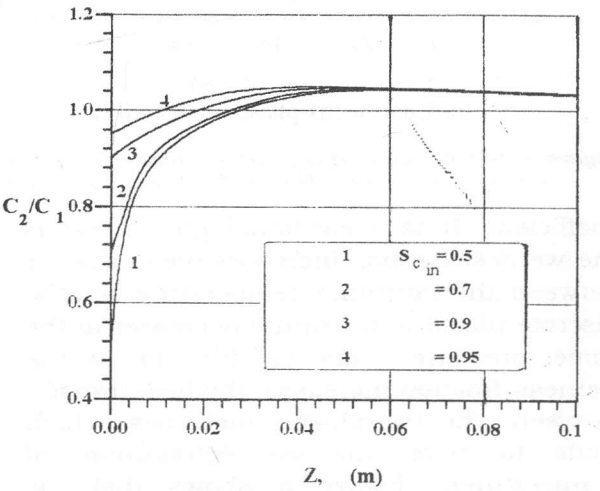

b- Effect of initial slip coefficient, ($S_{c_{in}}$)
($r_{d_{in}}$ = 2.5 μm , δ_d = 6° & y_{in} = 0.5)

Figure 3 Dimensionless velocity ratio (c_2/c_1) distribution along diffuser axis. (P_{in} = 6 bar, c_{in} =300m/s)

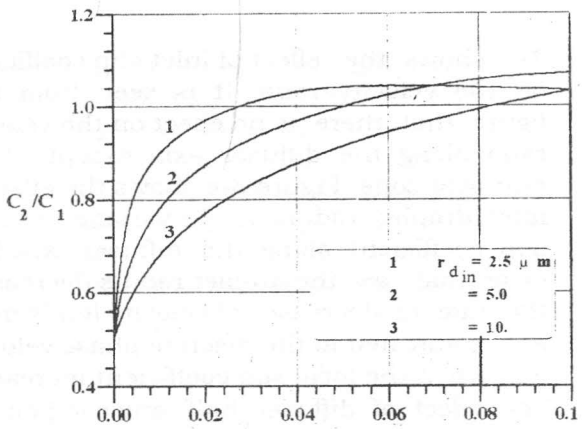

c- Effect of initial droplet radius, ($r_{d_{in}}$)
(δ_d = 6°, y_{in} = 0.5 & $S_{c_{in}}$ = 0.5)

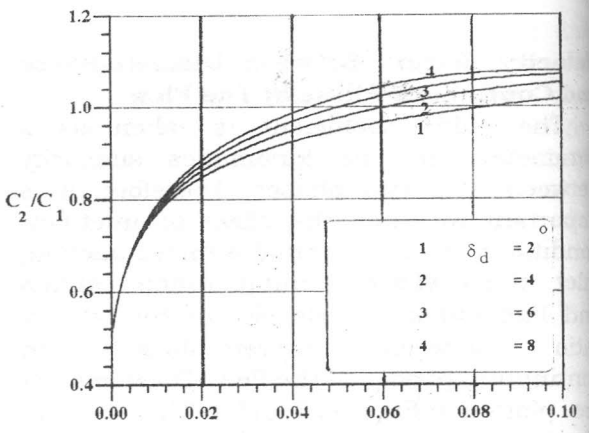

d- Effect of half diffuser angle, (δ_d)
($S_{c_{in}}$ = 0.5, y_{in} = 0.5 & $r_{d_{in}}$ = 5 μm)

Figure 3 (cont'd) Dimensionless velocity ratio distribution (c_2/c_1) along diffuser axis. (P_{in} = 6 bar, c_{in} =300m/s)

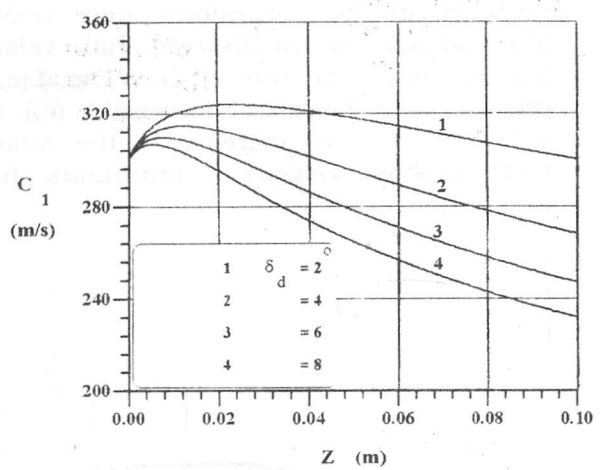

a- Continuous-phase velocity, (c_1)

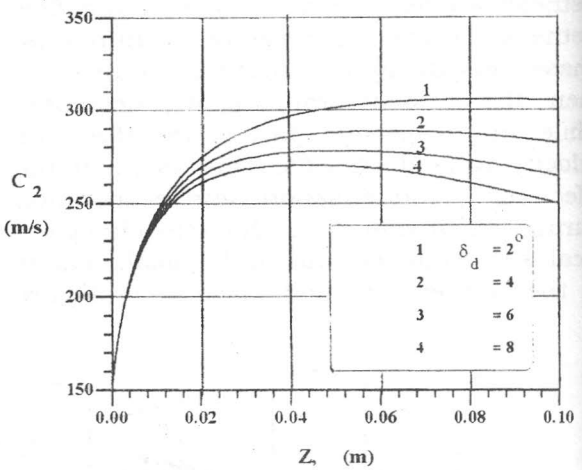

b- Discrete-phase velocity, (c_2)

Figure 4 Absolute continuous-phase and discrete-phase velocities distribution along diffuser axis.
(p_{in} = 6 bar, c_{in} = 300 m/s, $S_{c_{in}}$ = 0.5, y_{in} = 0.5 & $r_{d_{in}}$ = 2.5 μm)

coefficient. It is clear from Figure 5 that as the wetness fraction increases the difference between the saturation temperature and the discrete-phase temperature decreases at the same pressure. This is due to, as the wetness fraction increases, the heat transfer between the two-phases increases, which leads to more intensive equalization of temperatures. Figure 5 shows that, by increasing the half diffuser angle the temperature ratio T_2 (z)/T_s (z) increases.

Temperature Ratio

During expansion of two-phase flow through ducts, temperatures of continuous-phase T_1(z) and discrete-phase T_2 (z) are different from the saturation temperature T_s (z) at the same pressure. Therefore, it is important to determine the direction of heat transfer between the two phases. Figure 5 shows the variation of dimensionless discrete-phase temperature T_2 (z)/T_s (z) for different inlet wetness fraction and slip

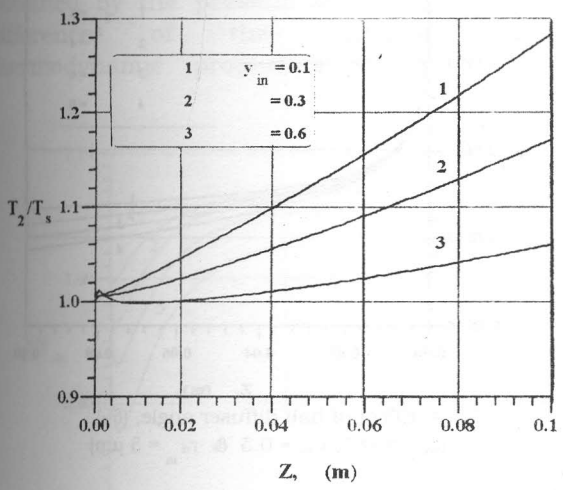

a- Effect of initial wetness fraction, (y_{in}).
($r_{d\,in}$ = 5 μm , $S_{c\,in}$ = 0.5 & δ_d = 6°)

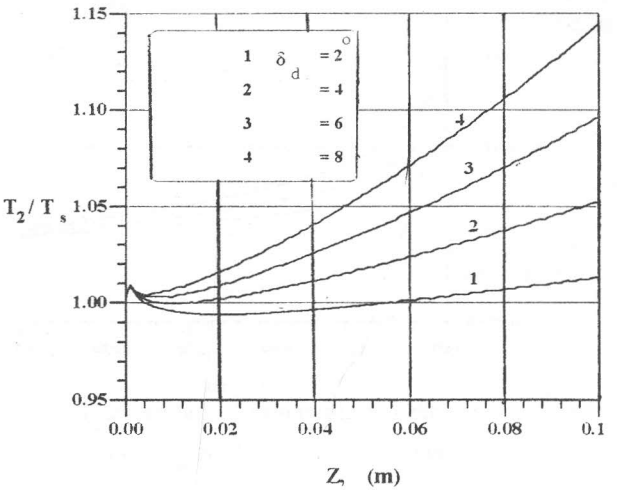

b- Effect of half diffuser angle, (δ_d).
($r_{d\,in}$ = 5 μm, $S_{c\,in}$ = 0.5 & y_{in} = 0.5)

Figure 5 Variation of discrete-phase temperature, (T_2) to corresponding saturation temperature, (T_s) along diffuser axis.
(p_{in} = 6 bar & c_{in} = 300 m/s)

Volumetric Concentration

The volumetric concentration of discrete-phase is in proportional relation with the wetness fraction and droplet radius, equation 40. Figure 6-a confirms this relation. Also it is seen from Figure 6-b, as the inlet slip coefficient increases the density ratio (ρ_2/ρ_1) decreases, this leads to an increase in volumetric concentration. Figure 6-c shows the effect of initial droplet radius on the variation of discrete-phase volumetric concentration. It is clear that, as the droplet radius increases the volumetric concentration of discrete-phase increases, on the other side the number of droplets in cubic meter decreases. This is because the volumetric concentration of discrete-phase and droplet radius are in proportional relation.

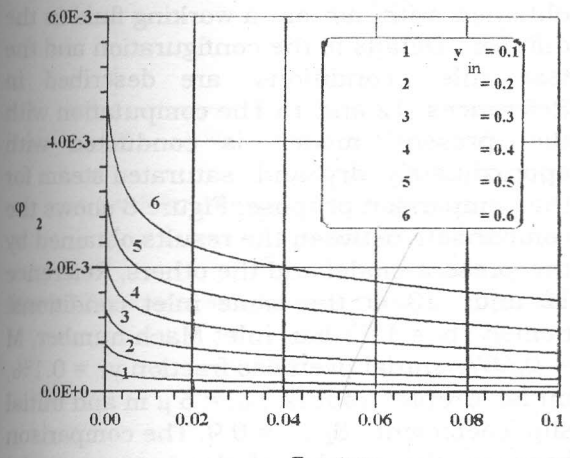

a- Effect of initial wetness fraction, (y_{in}).
($r_{d\,in}$ = 5 μm , δ_d = 6° & $S_{c\,in}$ = 0.5)

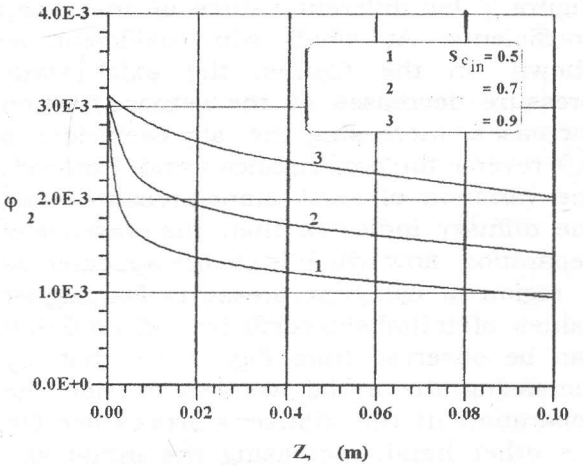

b- Effect of initial slip coefficient, ($S_{c\,in}$).
($r_{d\,in}$ = 2.5 μm ,δ_d = 6° & y_{in} = 0.5)

Figure 6 Variation of discrete-phase volumetric concentration, (φ_2) along diffuser axis.
(p_{in} = 6 bar and c_{in} = 300 m/s)

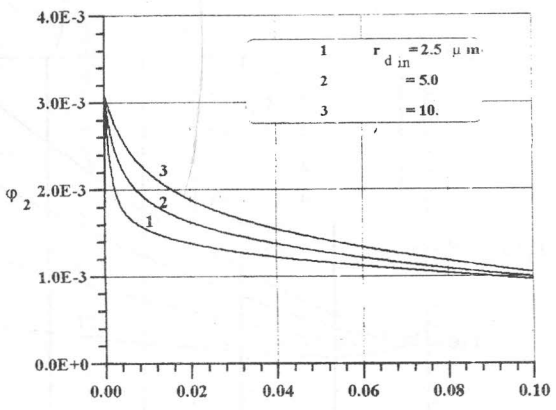

c- Effect of initial droplet radius, ($r_{d_{in}}$).
($\delta_d = 6°$, $y_{in} = 0.5$ & $S_{c_{in}} = 0.5$)

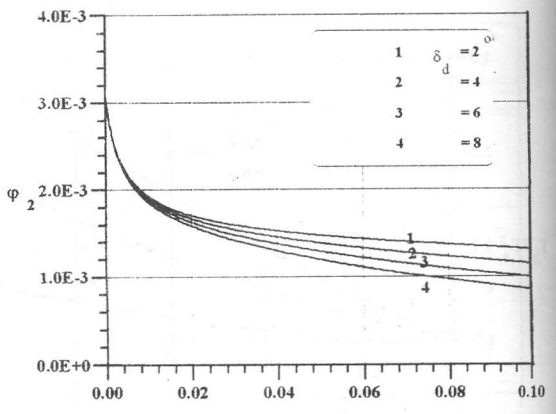

d- Effect of half diffuser angle, (δ_d).
($S_{c_{in}} = 0.5$, $y_{in} = 0.5$ & $r_{d_{in}} = 5$ μm)

Figure 6 (Cont'd) Variation of discrete-phase volumetric concentration, (φ_2) along diffuser axis.
(p_{in} = 6 bar and c_{in} = 300 m/s)

Validation of Numerical Model in Wide-Angle Diffuser

The numerical model was tested in case of separated flow through conical diffusers. A conical diffuser has a length of (0.5 m) and the total divergence angle was varied up to 16 degrees was examined. The computations were performed for different values of initial conditions such as, wetness fraction, slip coefficient and droplet radius to indicate the variation of these parameters on the diffuser performances in this case. The influence of initial wetness fraction on the axial static pressure along the diffuser axis is shown in Figure 7 for different values of initial slip coefficients. At small slip coefficient, as shown in the figures, the axial static pressure decreases as the wetness fraction increases. Increasing the slip coefficient to 0.9 reverse the performance trend. However, the variation of axial static pressure along the diffuser indicates that, the presence of separation flow which is clearly appeared as a region of constant pressure. For higher values of initial slip coefficient, (S_{in} = 0.9) it can be observed from Figure 7-c that, by increasing the initial wetness fraction the separation in the diffuser starts earlier. On the other hand, increasing the initial slip coefficient reduces the pressure drop at the diffuser entrance.

To verify the present model, computations are performed and compared with inviscid and viscid analytical solutions and available experimental results of References 12 and 13, respectively. The tested diffuser presented in Reference12 has a length of 0.2 m, non-dimensional length of 15.49 and 4.045 degrees half divergence angle with total area ratio of 9.14. As there is a sever shortage in experimental data for flow of wet steam through diffuser. Thus, the comparison is conducted with air flow as a working fluid through the diffuser. The available data in these references were obtained with air as a working fluid in the diffuser. Details of the configuration and the test inlet conditions are described in References 12 and 13 The computation with the present model is conducted with approximately dry and saturated steam for the comparison purpose. Figure 8 shows the comparison between the results obtained by the present model and the others, Reference 12 and 13 at the same inlet conditions, namely p_o = 1.27 bar, inlet Mach number, M = 0.667, initial wetness fraction y_{in} = 0.1%, initial droplet radius, r_{din} = 5 μ m and initial slip coefficient, $S_{c\ in}$ = 0.9. The comparison between the results of the present model and the others indicates that the trend is the same. It is observed from the comparison that, underestimated results

obtained by the present model due to the difference of the physical and thermodynamic properties of the tested working fluids, in addition to the separation possibility in the diffuser as mentioned in Reference13.

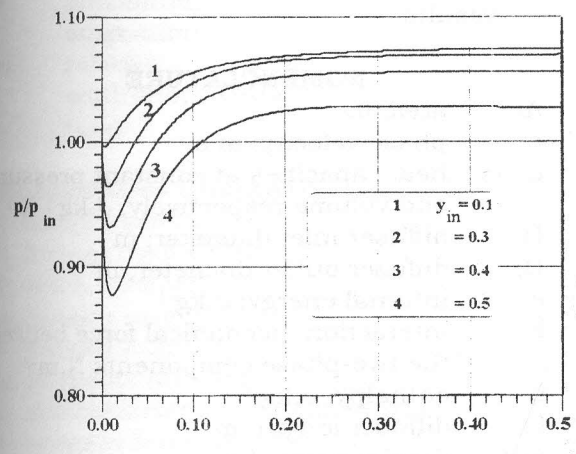

a- Effect of initial wetness fraction, (y_{in})
($\delta_d = 8°$, $r_{d_{in}} = 5$ μm & $Sc_{in} = 0.5$)

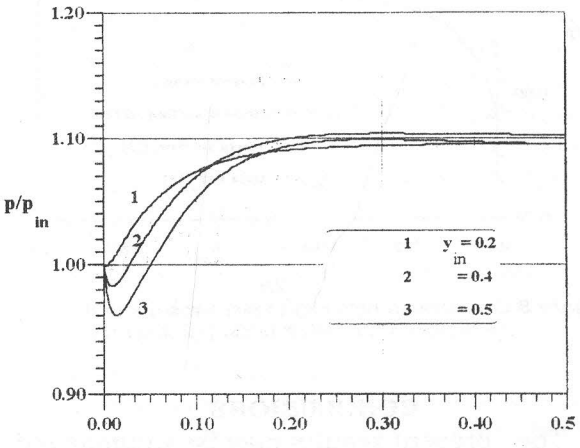

b- Effect of initial wetness fraction, (y_{in})
($\delta_d = 8°$, $r_{d_{in}} = 5$ μm & $Sc_{in} = 0.7$)

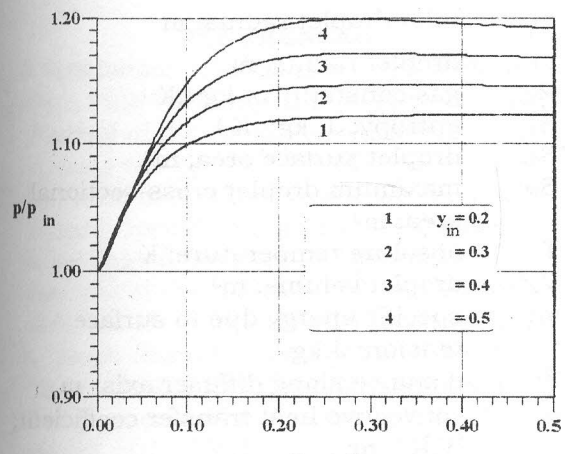

c- Effect of initial wetness fraction, (y_{in})
($\delta_d = 8°$, $r_{d_{in}} = 5$ μm & $Sc_{in} = 0.9$)

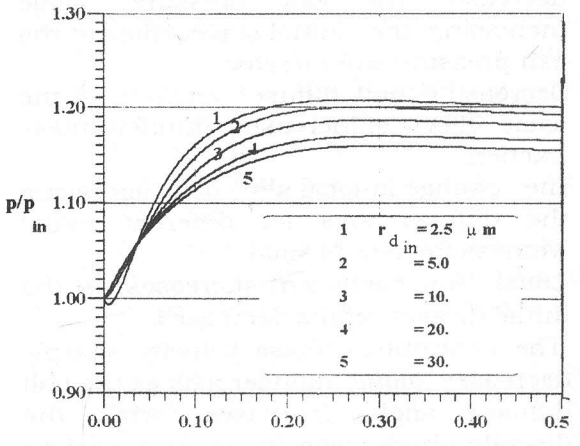

d- Effect of initial droplet radius, ($r_{d_{in}}$)
($\delta_d = 8°$, $y_{in} = 0.5$ & $Sc_{in} = 0.5$)

Figure 7 Dimensionless axial static pressure (p/p_{in}) distribution along diffuser axis ($p_{in} = 6$ bar & $c_{in} = 300$ m/s)

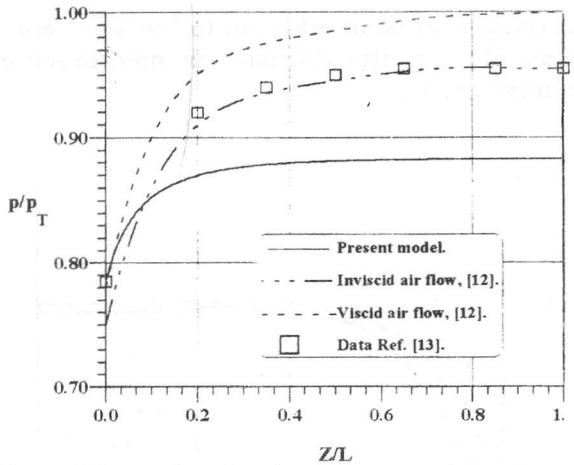

Figure 8 Comparison between present results and published data References, [12 and13].

CONCLUSIONS

The present results may be summarized as follows:

1- In general the diffuser performance is affected by the inlet flow conditions. Increasing initial wetness fraction will decrease the exit pressure, while increasing the initial slip coefficient the exit pressure will increase.

2- Decreasing half diffuser angle gave the same effect of increasing initial wetness fraction.

3- The change in local slip coefficient along the diffuser axis for different initial wetness fraction is small.

4- Local slip coefficient increases as the initial droplet radius decreases.

5- The continuous-phase velocity sharply decreases along diffuser axis as the half diffuser angle increases, while the discrete-phase velocity is in a slightly decrease.

6- As the initial wetness fraction increase; the temperature difference between discrete-phase temperature and corresponding saturation temperature decreases.

7- The presence of negative pressure gradient, (first part of the channel acts as a nozzle) may lead to a critical feature and depends upon the initial dryness fraction and slip coefficient.

8- The comparison between the results of the present model and the other experimental and theoretical models revealed that the present model has the same trend but underestimate the results.

NOMENCLATURE

A: area; m^2
c: phase velocity; $m.s^{-1}$
c_p, c_v heat capacities at constant pressure and volume respectively; $J.kg^{-1} K^{-1}$
D_1: diffuser inlet diameter; m
D_2: diffuser outlet diameter; m
e: internal energy; $J.kg^{-1}$
F: interaction mechanical force between the two-phase components $N.m^{-3}$
i: enthalpy; $J.kg^{-1}$
L: diffuser length; m
m_d: droplet mass; kg
p: pressure; Pa
Q: heat release per unit volume; $J.m^{-3}.s^{-1}$
q: conductive heat transfer rate per unit area; $Jm^{-2} s^{-1}$
$r_{d_{in}}$: inlet droplet radius; m
r_d: droplet radius; m
R_B: gas constant; $J. kg^{-1}.K^{-1}$
S: entropy; $J. kg^{-1}.K^{-1}$
S_d: droplet surface area; m^2
S_M: maximum droplet cross-sectional area; m^2
T: absolute temperature; K
V_2: droplet volume; m^3
v_s: specific energy due to surface tension; $J.kg^{-1}$
Z: distance along diffuser axis; m
α: convective heat transfer coefficient; $W.K^{-1}. m^{-2}$
σ: surface tension coefficient; $N.m^{-1}$
ρ: density; $kg.m^{-3}$
μ: Gibbs function; $J. kg^{-1}$
ν: kinematic viscosity; $m^2 s^{-1}$
χ: phase conversion rate; $kg.m^{-3}.s^{-1}$
λ: thermal conductivity; $W.K^{-1}.m^{-1}$
δ_d: diffuser half angle degree

Subscripts

1: continuous-phase;
2: discrete-phase;
c: condensation;

d: droplet;
e: evaporation;
ig: ideal gas;
in: inlet;
M: maximum;
o: stagnation;
rel.: relative;
s: saturation, surface;
T: total;

Dimensionless Quantities

B: compressibility;
C_f: friction coefficient;
M: Mach number;
Nu: Nusselt number;
Pr: Prandtl number;
Re: Reynolds number;
S_c: slip coefficient and defined by c_2/c_1;
y: wetness fraction;
α_c: condensation coefficient;
α_e: evaporation coefficient;
γ: specific hear ratio;
φ: volumetric concentration;

REFERENCES

1. P. Bradshaw, "Performance of a Diffuser With Fully-Developed pipe Flow at Entry", Journal of the Royal Aeronautical Society Volume 66, pp. 733, (1962).
2. Riccardo Sala, Pier Luigi Vivarelli and Gianni Garuti, "Numerical Analysis of wide-angled Diffuser in Turbulent Flow", Journal of the hydraulics Division, Vol. 106, No. HY 5, pp. 629-647 May (1980).
3. K. Singh Rakesh, "Asymptotic Velocity Detect Profile in An Incipient-Separating Axisymmetric Flow", AIAA Vol. 33, No. 1, pp. 94-101, (1995).
4. J.E Hench and J.P Johnston, "Two-Dimensional Diffuser Performance With Subsonic, Two-Phase, Air-Water Flow", Transactions of the ASME, Journal of Basic Engineering, Vol. 107, pp. 105-121, (1972).
5. Tomitaro Toyokura and Kenichi Suzuki, "Performance of Vertical Diffuser for Air-Water Mixture", Bulletin of JASME, Vol. 29, No. 252, pp. 1765-1769, (1986).
6. J.L. Livesey and A.O. Odukwe, "Some Effects on Conical Diffuser Performance of Preceding Normal Shock Boundary-Layer Interaction", Proc. Instn. Mech. Engrs., Vol. 188, pp. 56-74, (1974).
7. Danelen, V.C., Tsiklauri, J.V. and Seleznev, L.I., "Adiabatic Two-Phase Flow", Moscow; Atom publishers, (1973).
8. D.D. Kladas and D.P. Georgiou, "A relative Examination of C_D-Re Relationships Used in Particle Trajectory Calculations", Transactions of the ASME, Journal of Fluids Engineering, Vol. 115, pp. 162-165, (1993).
9. V.P. Isachenco, V.A., Osipova and A.S., Sukomel, "Heat Transfer", Mir Publishers Moscow, (1977).
10. M H. Hamed, "Investigation of Unsteady Two-Phase Flow of Wet Steam Through Nozzles", Alexandria Engineering Journal. Vol. 37, No. 5, A237-A249, (1998).
11. C.A.J. Fletcher, "Computational Techniques For Fluid Dynamics", second edition Springer-Verlag, Sydney, (1991).
12. W.W. Bower "Analytical Procedure for Calculation of Attached and Separated Subsonic Diffuser Flows", J. AIRCRAFT, Vol. 13, No. 1, pp. 49- 56, (1976).
13. J.I. Means, P.C. Glance and H.A.Klassen, H.A., "Analytical Investigation of Conical Diffusers", NACA TMX-2065, Aug. (1972).

Received March 10. 1999
Accepted August 28. 1999

السريان ثنائى الطور فى النواشر

مفرح حمادة حامد

قسم هندسة القوى الميكانيكية – جامعة المنوفية

ملخص البحث

تصف هذه الورقة النموذج النظرى لحل السريان ثنائى الطور (البخار الرطب) أحادى البعد المستقر فى النواشر. وتشمل هذه الدراسة تأثير الظروف الابتدائية مثل معامل الانزلاق و نسبة الرطوبة و نصف القطر المبدئى للقطرة وكذا المتغيرات الهندسية للناشر على أداء الناشر. وللتنبؤ ومعرفة كل من بارامترات الطور الأول (السريان المتصل) و بارامترات الطور الثانى (السريان الغيرمتصل) تم استخدام طريقة (رونج كوتا) فى حل النموذج النظرى. وقد أظهرت النتائج التى تم الحصول عليها من دراسة سريان البخار الرطب خلال الناشر أنه توجد تغيرات فى أداء الناشر و أن هذا الأداء يعتمد على التأثيرات المتبادلة بين كل من الطورين. كما أظهرت النتائج أن أداء جزء من الناشر كبوق قد يؤدى إلى وجود ظروف حرجة أثناء السريان وأن وجود هذا الجزء يتوقف على نسبة الرطوبة. وقد تم عقد مقارنة بين النتائج التى تم الحصول عليها من النموذج الرياضى الحالى لسريان بخار جاف مشبع خلال ناشر مع بعض النتائج النظرية و المعملية المتاحة و المنشورة لسريان الهواء خلال نفس الناشر. وأظهرت هذه المقارنة توافقا نوعيا مقبولا.